The crystal field concept (CFC) in geosciences: Does the crystal field stabilization energy of Cr^{3+} rule its intercrystalline partitioning behavior?

K. LANGER and M. ANDRUT*

Institute of Mineralogy and Crystallography, Technical University, D-10623 Berlin, Germany

Abstract—According to crystal field concepts, CFC (BURNS, 1970a and 1993), $3d^N$-ion partitioning between different phases in geochemical systems or between different structural sites in multisite phases is governed by the crystal field stabilization energies of the $3d^N$-ions within the coexisting phases or the different sites, respectively. Although CFC was qualitatively shown to be valid in many systems, other authors claim that ionic sizes and distances within the polyhedra incorporating the $3d^N$-ions play a more important role. A decision over CFC and this latter predominantly geometrical concept may be taken when quantitative relations of the type

$$c_{3d^N} = f(CFSE_{3d^N}) \text{ or } K_{D,3d^N,(p,T)}^{(Ph1/Ph2)} = f(\Delta CFSE_{3d^N}^{(Ph1 - Ph2)})$$

with positive f are found. Such quantitative relations may be seen when influences of different bulk chemistry and p,T-conditions during formation on c_{3d^N} are ruled out. Therefore, we determine c_{3d^N} and $CFSE_{3d^N}$, for the case of Cr^{3+}, on coexisting minerals in the following parageneses, which contain Cr^{3+} above the trace level (>1000 ppm): 1 and 2: Gt/Cpx/Ky, grosspydite Zagadochnaya/ Yakutia; 3: Gt/Cpx/Amph, eclogite Urals/Russia; 4: Cor/Parag/ Phlog, Raj Iz/Antarctica; 5: Cor/Ky/ Fuchs, Mysore/India; 6: Cor/Amph, Longido/Tanzania; 7: Opx/Cpx, Cpx exsolution in Opx from an eclogite Urals/Russia. The results quantitatively confirm CFC for parageneses 1 through 6. In case of paragenesis 7, a negative correlation between c_{Cr3+} and $CFSE_{Cr3+}$ was observed. This deviation from CFC can be explained on the basis of crystallochemical arguments.

INTRODUCTION

Outline of the Crystal Field Concept, CFC

THE d-ELECTRONS of $3d^N$-ions in the gaseous state are subject to the spherical fields of their nuclei and, therefore, are degenerate with respect to both energy and symmetry. When incorporated into nonspherical fields, e.g., ligand fields of regular or distorted octahedra in a mineral structure, the degeneracies are at least partly lifted. The respective spectroscopic states of the $3d^N$-ions are split to produce an electronic ground state and concomitant excited state or states. This effect is called crystal field splitting. It is characterized by the crystal field parameter 10Dq, or in the case of octahedral fields, $10Dq_{oct.}$. These relations are outlined in Fig. 1, which presents the octahedral crystal field splittings of geochemically important $3d^N$-ions with total d-electron numbers N between 1 and 9.

For the same $3d^N$-ion ligand-distances, the crystal field parameters behave as

$$10Dq_{oct} : 10Dq_{cub} : 10Dq_{tetr} = 1 : \left(-\frac{8}{9}\right) : \left(-\frac{4}{9}\right) \quad (1)$$

in cubic and tetrahedral fields[1].

In the splitting schemes of the lower part of Fig. 1, the spectroscopic ground states of the free ions are represented by symbols derived from Russell-Saunders- or LS-coupling, $^{(2S+1)}L_J$, of the d-electrons. The crystal field split states are characterized by the symbols of the irreducible representations of their symmetry (cf. e.g. MCCLURE, 1958; DUNN et al., 1965; SCHLÄFER and GLIEMANN, 1980).

One essential aspect of all the splitting schemes shown in Fig. 1 is that the electronic ground states in the crystal field are energetically lower than the spectroscopic states of the free ions from which they originate. This energy gain of the $3d^N$-ions on incorporation into a crystal field is called crystal field stabilization energy, CFSE, and is indicated for the case of an octahedral field in Fig. 1 by multiples of Dq for all $3d^N$-ions $1 \leq N \leq 9$.

The crystal field stabilization energy in octahedral fields, point group O_h, is obtained from

$$-CFSE_{3d^N,oct} = [4n - 6(N - n)] \cdot Dq \quad (2)$$

or from

$$-CFSE_{3d^N,tetr,cub} = [6n - 4(N - n)] \cdot Dq \quad (3)$$

for tetrahedal or cubic fields of point group T_d or O_h, respectivly. N is the total number of d-electrons and n is the d-electrons in the crystal field-derived ground state (t_{2g} in octahedral fields

*Present adress: GeoForschungszentrum Potsdam, Telegraphenberg, D-144407 Potsdam, Germany.

[1]The − sign is a consequence of the reversal of electronic states compared to their sequence in octahedral fields.

d^1		d^2		d^3		d^4		d^5		d^6		d^7		d^8		d^9	
Ti^{3+}		V^{3+}		Cr^{3+}		Mn^{3+}		Fe^{3+}		Co^{3+}							
				V^{2+}		Cr^{2+}		Mn^{2+}		Fe^{2+}		Co^{2+}		Ni^{2+}		Cu^{2+}	
^2D		^3F		^4F		^5D		^6S		^5D		^4F		^3F		^2D	
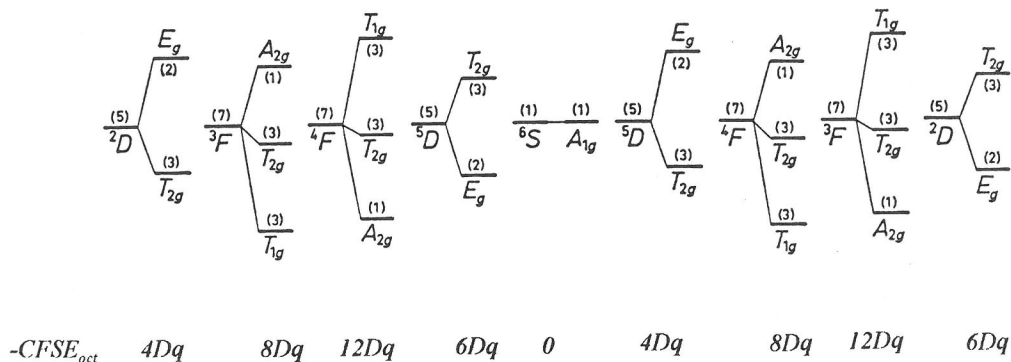
FIG. 1. d-electron configurations, spectroscopic ground states, $^{(2S+1)}L_J$, of the free ion case, crystal field-splitting of these free ion ground states as well as crystal field stabilization energies of the whole series of $3d^N$-ions in an octahedral environment, point group O_h (after SCHLÄFER and GLIEMANN, 1980; in case of d^2 and d^7, 6Dq was corrected to 8Dq). The ordinate in the split level diagrams is energy in arbitrary units. For further explanations *cf.* text.

or e_g in tetrahedral and cubal fields for the one electron case.)

In addition to the type and symmetry of the coordination polyhedra, two peculiarities of the crystal field determine the crystal field splitting parameter 10Dq of a given $3d^N$-ion,

(i) *The nature of the ligands:* In the case of rock forming-minerals and related geochemical systems, these are predominantly O^{2-}, OH^-, H_2O, F^-, and S^{2-}. Generally, 10Dq increases within the ''spectrochemical series'' (TSUCHIDA, 1938a, b, and c; SHIMURA and TSUCHIDA, 1956) which for the just mentioned ligands is $F^- < OH^- < O^{2-} < H_2O < S^{2-}$ (BURNS, 1993).

(ii) *The mean $3d^N$-ion ligand-distance:* In the case of octahedral fields of ligands with effective charge Z_L, crystal field theory yields

$$10Dq_{oct} = \frac{5}{3} \frac{(Z_L \times e^2)}{R^5} \times \overline{r^4} \qquad (4)$$

(*e.g.,* DUNN *et al.,* 1965; LEVER, 1968), wherein $\overline{r^4}$ = mean fourth power radius of the d-electrons of the central ion, a quantity that is thought to be approximately constant for $3d^N$-ions of the same valence, and R = the mean cation-ligand distance.

On decendent symmetry from O_h or T_d, the rem-

nant degeneracies of states are gradually removed, leading to further splitting of the E- and T-states, shown in Fig. 1. When ground states are subject to such low symmetry splitting, as is the case for all $3d^N$-ions except for $3d^3$, $3d^5$, and $3d^8$ (*cf.* Fig. 1), then the resulting ground state is lowered again compared to the high symmetry case. Consequently, $CFSE_{3d^N}$ is higher at such sites for $3d^N$-ions with degenerate crystal field ground state.

The energy gaps between the ground and excited crystal field states of Fig. 1, eventually split by low symmetry, are in the range of 25000 to 4000 cm^{-1}, corresponding to 3.1 to 0.5 eV. This means that they occur in the UV to NIR spectral region with wavelengths of 400 to 2500 nm. Electronic resonant absorption spectroscopy within the aforementioned region is used to measure such energies and to extract 10Dq and, from this $CFSE_{3d^N}$. Polarized radiation and crystallographically oriented crystal slabs are necessary in the case of anisotropic crystals where symmetry related selection rules for the electronic transitions are active.

The importance of these crystal field considerations and their experimental evaluation is obvious from the following: in the early fifties, it was shown that the heat of hydration of $3d^N$-ions as well as

the lattice energy of $3d^N$-metal sulfides can only be correctly calculated when the crystal field stabilization energy of the $3d^N$-ions was included into the calculations that were based on the electrostatic approach, valid for spherical ions with $3d^0$-configuration.

This result stimulated many geoscientists to suggest that the crystal field stabilization energy, $CFSE_{3d^N}$, should also affect or even rule the thermodynamic properties of $3d^N$-ion bearing minerals and the behavior of $3d^N$-ions in homogeneous or inhomogeneous geochemical systems, *e.g.*, their intra- and intercrystalline distribution behvior and their partitioning between crystals and melt (WIL-LIAMS, 1959; BURNS and FYFE, 1964, 1966, 1967a and b; BURNS *et al.*, 1964; CURTIS, 1964; MERLINO, 1965; SCHWARCZ, 1967; STRENS, 1968; BURNS, 1968, 1970a, and 1976; BURNS and SUNG, 1978). This approach was further stimulated by the pioneering book of BURNS (1970b, 1993).

Considering $3d^N$-ion distributions, different $CFSE_{3d^N}$ in phases with different cation-ligand distances and different site symmetries may force the $3d^N$-ions predominantly into one of the phases in multiphase assemblages. This concept to interpret interphase distribution is called crystal field concept, CFC, throughout the paper. It predicts that $3d^N$-ions fractionate into those sites and/or phases wherein $CFSE_{3d^N}$ is highest (BURNS, 1970b, 1993).

THE PROBLEM AND AN APPROACH TO SOLVE IT

CFC proved capable of qualitatively interpreting geochemical observations on $3d^N$-ion partioning between melt and crystals, between coexisting minerals in magmatic and metamorphic rocks from the earth's crust and mantle between different structural sites in multisite mineral structures, or solid solution thermodynamics and phase transitions of $3d^N$-ion bearing minerals. This was comprehensively presented 1970 and 1993 by Roger BURNS.

Despite the abundant qualitative evidence for the validity of CFC, concepts based on ionic radii and site geometry in mineral structures are often thought to be superior in the interpretation of partitioning patterns of not only the spherical $3d^0$-ions but also of nonspherical $3d^N$- or $4f^N$-ions (*e.g.*, JEN-SEN, 1973; BEATTIE, personal comm.). The argument for this is that the Madelung part of the lattice energy of crystals is much higher than any crystal field effects therein. However, this may be true only for trace amounts of $3d^N$-ions but not for solid solutions with concentrations of $3d^N$-ion end members higher than 1 to 2 mole%, because $CFSE_{3d^N}$ typically has values between 50 and 260 [KJ/g-

ion] depending on the type of $3d^N$-ion and of its structural site.

The problem is, thus, to decide between CFC and the just mentioned geometrical approach in the case of $3d^N$-ion partioning in a concentration range above the trace level. This problem can only be solved by checking for *quantitative* relations between $3d^N$-ion concentrations and $CFSE_{3d^N}$

$$C_{Cr^{3+}} = f(CFSE_{Cr^{3+}}) \qquad (5)$$

or between distribution coefficients and differences in the crystal field stabilization energies

$$K_{D,Cr^{3+}(p,T)}^{Ph1/Ph2} = f(\Delta CFSE_{Cr^{3+}}^{Ph1 - Ph2}) \qquad (6)$$

Such quantitative relations may be found only when any effects of the bulk chemistry and of temperature and/or pressure changes on the partitioning of $3d^N$-ions in the respective geochemical system, *e.g.*, between the minerals of a rock, can be ruled out. Therefore, our approach is to obtain $CFSE_{3d^N}$ and c_{3d^N} for coexisting, homogeneous minerals. Results of such work are presented here for the case of Cr^{3+} in paragenetic minerals (*cf.* ANDRUT, 1995). The behavior of this $3d^3$-ion was studied because its $CFSE_{Cr^{3+}}$ is highest among the geochemically significant $3d^N$-ions and because its ground state in octahedral crystal fields, strongly preferred by this ion (BURNS, 1970b and 1993), is nondegenerate (*cf.* Fig. 1). Furthermore, the energy of the spin-allowed transition $^4A_{2g} - {}^4T_{2g}$ of $Cr^{3+[6]}$ (Fig. 1) is equal to $10Dq_{oct}$ (TANABE and SUGANO, 1954 and b).

SAMPLES AND METHODS

Crystal fragments of coexisting minerals with suitable grain size were drilled out of a series of chromium containing rocks, compiled in Table 1.

For measurement of polarized single crystal spectra, anisotropic mineral crystals were oriented by means of spindle stage techniques (BLOSS, 1981) such that one of the main directions of their indicatrix, either X, Y, or Z (notation of TRÖGER, 1952), became the rotation axis. Two crystal fragments of each of the coexisting minerals were prepared to facilitate measurements with E parallel to X, Y and Z. The oriented crystals were embedded and ground to obtain the suitable thickness, then polished from both sides. Quartz crystals oriented parallel to *c*, placed aside the crystals to be studied, served to determine the thickness of the mounts by evaluating the birefringence of quartz. In this way, single crystal slabs with thicknesses between 50 and 500 μm and containing the main optical directions (Y,Z), (X,Z), or (X,Y), respectively, were obtained. The procedures of preparation and thickness measurements are described elsewhere (LANGER, 1988). The slabs had lateral dimensions between about 200 and 900 μm. Their orientation was checked by conoscopic observations, and is thought to be correct to within 3° to 5° for

Table 1. Parageneses studied and their sources. Abbreviations: Gt = garnet, Kpx = clinopyroxene, Opx = orthopyroxene, Ky = kyanite, Amph = clinoamphibole, Ru = corundum (ruby), Parag = paragonite, Phlo = phlogopite, Fu = fuchsite.

Pargeneses studied	Symbols used for minerals studied	Source	Obtained from
Garnet Clinopyroxene Kyanite	Zag C1-Gt, Zag G1-Gt[1] Zag C1-Cpx, Zag G1-Cpx Zag C1-Ky, Zag G1-Ky	Grosspydite xenolith Z13, Zagadochnaya, Yakutia	N.V. Sobolev, Novosibirsk, Russia
Garnet Clinopyroxene Clinoamphibole	MC1-A Gt MC-1A Cpx MC1-A Amph	Eclogite MC1, Urals, Russia	A.N. Platonov, Kiev, Ukraine
Corundum Paragonite Phlogopite	RI Ru RI Parag RI Phlo	Raj Iz, Antarctica	A.N. Platonov, Kiev, Ukraine
Corundum Kyanite Fuchsite	My Ru My Ky My Fu	Mysore, India	S. Herting-Agthe, Techn. Univ. Berlin
Corundum Clinoamphibole	Lon Ru Lon Amph	Amphibolite Longido, Tanzania	S. Herting-Agthe, Techn. Univ. Berlin
Clinopyroxene Orthopyroxene	OPXCPX-Cpx OPXCPX-Opx	Exsolution of clinopyroxene in orthopyroxene from an eclogite, Urals	A.N. Platonov, Kiev, Ukraine

[1]Two sets of the minerals garnet, clinopyroxene, and kyanite were extracted from the grosspydite xenolith, C1 and G1.

observation in the green part of the spectrum. In the case of OPXCPX-Kpx (Table 1), *i.e.,* the clinopyroxene lamellae exsolved from orthopyroxene at an orientation independent from that of orthopyroxene could not be achieved. The orthopyroxene slab was oriented parallel to Y, hence E//X and E//Z spectra could be measured on Opx. The indicatrix of the clinopyroxene lamellae is tilted against that of Opx. Therefore, the clinopyroxene spectra were, in this case, polarized E// ca.X and E// ca.Y. However, this will not greatly influence 10Dq, as the baricenter of the $^4A_{2g} - {}^4T_{2g}$ transition does not strongly depend on the polarization.

Polarized single crystal spectra, $\log(I_o/I) = f(\bar{\nu})$, in the spectral range 40000 to 4000 cm^{-1} were scanned in a single-beam microscope spectrometer (Zeiss UMSP 80) using UV-transparent 10× objectives (Zeiss ULTRA-FLUAR) as condenser and objective. Details of the procedure are given elsewhere (LANGER and FRENTRUP, 1979; LANGER, 1988). Luminous field and measuring diaphragms were 80 and 32 μm, respectively, in the UV/VIS or 100 and 60 μm, respectively, in the NIR. Spectral band widths and step widths were 1 nm each in the UV/VIS or 8 and 10 nm, respectively, in the NIR. Spectra were obtained as averages of up to 200 scans, the reference $I_o = f(\bar{\nu})$ being obtained in the quartz plate (see above). Special care was used to select optically clear measuring spots on the crystal slabs studied. Curve deconvolution and band positions were achieved by means of a peak fit program, assuming Gaussian functions to represent the component bands in complex spectra.

Microprobe analyses on a variety of different points on each crystal were performed on a Cameca Camebax in the ZELMI laboratory of the Technical University Berlin subsequent to the spectral measurements. To check for the homogeneity of the crystals studied, N repeated analy-

ses on M various points on a grain were performed. From these, standard deviations were calculated for the means of N_i analyses of one individual point i as well as of all N analyses on M points. When the standard deviation of the mean of all N measurements on M points on a grain does not exceed 2s of N_i measurements on one individual point i, there is no significant compositional inhomogeneity with respect to the elements measured in the crystal grain.

X-ray diffraction. For data evaluation, the molar volumes, V_M in [dm^3], of the minerals under study were needed (see below). These data were calculated from the volumes of the unit cells, V_e in [A^3], by

$$V_M = \frac{10^{-27} \times V_e \times N_L}{Z} \qquad (7)$$

($N_L = 6.022*10^{23}$ mole^{-1}, Z = number of formula units per unit cell). Cell volumes were obtained from the lattice constants determined from powders prepared from a number of additional crystals extracted from the rock samples in addition to the coexisting ones, which had been prepared for spectroscopy and subsequent microprobe. The powder diffractograms were scanned on a Huber Guinier diffractometer G 645 (courtesy W. DEPMEIER, University of Kiel), using silicon as external standard.

EXPERIMENTAL RESULTS AND THEIR EVALUATION

Composition of the coexisting minerals studied

The crystallochemical formulae of the coexisting minerals studied as well as their lattice constants

are presented in Table 2. The crystallochemical formulae were calculated from the wt% values of the oxide components. These values were calculated as the averages of repeated measurements on several spots on the respective crystal slab, including the spot on which the spectral measurements had been performed. From a comparison of the standard deviations of mean values of repeated analyses on one spot with those obtained by averaging the data measured on several points on one slab, there was no indication of significant zoning or other chemical inhomogeneities of the minerals studied. Typical examples of such standard deviations are those of wt% Cr_2O_3 in kyanite from the Zagadochnaya parageneses C1 and G1 (*cf.* Table 1):

ZagC1-Ky:

n = 3 measurements on the same spot :
2.17%, s=0.06%

measurements on M = 7 different spots :
2.20%, s=0.09%

ZagG1-Ky:

n = 3 measurements on the same spot :
1.78% s=0.05%

measurements on M = 7 different spots :
1.83%, s=0.09%

From this, it may be estimated that the uncertainty in $n_{Cr^{3+}}$, *i.e.* the number of Cr^{3+}-ions per formula unit, of the formulae in Table 2 occurs in the third decimal point. This is important to note, as $n_{Cr^{3+}}$ will be used to calculate the volume-normalized chromium concentrations held by the coexisting phases (see below).

The spectra and the extraction of $10Dq_{cr3+}$ from them

As shown in the introduction, the crystal field parameter $10Dq_{Cr^{3+}}$ is equal to the lowest-energy spin-allowed electronic transition of Cr^{3+}, $A_{zg} - {}^4T_{2g}(F)$. This transition occurs in the absorption spectra of Cr^{3+}-bearing, oxygen-based structures as strong, broad band, centered between about 18500 and 15500 cm^{-1}, depending on the properties of the crystal field in the respective structural sites as described by eqn. (4). The half widths of this band range up to about 2500 cm^{-1}.

Examples of such spectra, measured during this study on coexisting Cr^{3+}-bearing garnet, clinopyroxene and kyanite, extracted as paragenesis G1 from the Zagadochnaya grosspydite xenolith, are shown in Figs. 2 to 5. It would go beyond the scope

of this paper to present the spectra measured on all the crystals studied (Table 1 and 2) and all parameters extracted. This will be the aim of a forthcoming paper (ANDRUT and LANGER, in preparation). Here, we shall concentrate on the problems of the extraction of 10Dq, using Figs. 2 to 5 as examples.

All the minerals studied contain Cr^{3+} in coordination octahedra with site symmetries lower than $O_h - m3m$. For example, in garnet, the octahedra have site symmetry $\bar{3}$, in corundum 3, in clinopyroxene M(1) 2 and in kyanite 1. As pointed out in the introduction, fields of lower symmetry than $O_h - m3m$ give in principle rise to two effects, important in the extraction of correct $10Dq_{Cr^{3+}}$-values:

(i) splitting of the excited, triply degenerate T(F) states of Cr^{3+} and

(ii) symmetry-related selection rules for the respective transitions between the nondegenerate crystal-field ground state of Cr^{3+} and the now nondegenerate excited states, originating from the aforementioned T-states by low-symmetry splitting. Such symmetry-related selection rules make allowance for a transition only, when the electric field vector of the exciting radiation has a special orientation with respect to the electric dipole moment vector of the transition considered (*cf. e.g.* WILSON *et al.,* 1955; COTTON, 1971).

The latter effect causes the "pleochroism" of crystals of low-symmetry minerals and other crystalline material. Other effects may contribute in the case of chemically complex natural minerals. For example, charge-transfer phenomena, may also give rise to strongly polarized absorption bands (SMITH and STRENS, 1976).

A third effect that eventually makes the extraction of $10Dq_{Cr^{3+}}$ from the spectra difficult is:

(iii) band-overlap of the $({}^4A_{2g} - {}^4T_{2g})$-derived Cr^{3+}-transition, or transitions respectively, by other excitations occurring in chemically complex natural minerals.

An example of (i) is the splitting of the two spin-allowed Cr^{3+}-bands in the clinopyroxene spectra of Fig. 4. This splitting, as well as the band polarizations (ii) that are obvious in Fig. 4, was interpreted to be caused by the nonregular symmetry of the Cr^{3+}-containing M(1)-octahedra of the clinopyroxene structure, the effects (i) and (ii) being most consistent with a $D_{2d} - \bar{4}2m$ pseudosymmetry (ABS-WURMBACH *et al.,* 1985). Another example of effect (ii) is the polarization of band intensities in the kyanite spectra of Fig. 3. An example of effect (iii) is the overlap between the $({}^4A_{2g} - {}^4T_{2g})$-derived Cr^{3+}-band in the kyanite spectra of Fig. 3 with a band originating from $Fe^{2+} - Ti^{4+}$ charge-

Table 2. Chemical composition, recalculated to crystallochemical formulae, and lattice constants of the paragenetic minerals studied. Compositions are averages of data calculated from microprobe analyses on a variety of spots on the respective crystal slab.

| Crystals	Analyzed composition	a [A]	b [A]	c [A]	[°]	[°]	[°]
ZagC1-Gt	$(Ca_{1.65}Mg_{0.75}Mn_{0.01}Fe_{0.62})^{[8]} (Al_{1.92}Cr_{0.09}Ti_{0.01})^{[6]} [SiO_4]_3$	11.649(4)					
ZagC1-Cpx	$(Ca_{1.60}Na_{0.35})^{[8]} (Mg_{0.52}Fe_{0.06}Al_{0.43}Cr_{0.03})^{[6]} [Si_{1.93}Al_{0.07}O_6]$	9.87(5)	8.61(5)	5.24(2)		106.0(4)	
ZagC1-Ky	$(Al_{1.95}Cr_{0.04}Fe_{0.01})^{[6]} [O/SiO_4]$	7.113(6)	7.860(5)	5.570(5)	90.11(8)	101.96(8)	105.89(7)
ZagG1-Gt	$(Ca_{1.62}Mg_{0.80}Mn_{0.01}Fe_{0.60})^{[8]} (Al_{1.92}Cr_{0.08}Ti_{0.02})^{[6]} [SiO_4]_3$	11.649(4)					
ZagG1-Cpx	$(Ca_{1.60}Na_{0.35})^{[8]} (Mg_{0.48}Fe_{0.06}Al_{0.44}Cr_{0.02})^{[6]} [Si_{1.95}Al_{0.05}O_6]$	9.87(5)	8.61(5)	5.24(2)		106.0(4)	
ZagG1-Ky	$(Al_{1.90}Cr_{0.04}Fe_{0.01})^{[6]} ([O/SiO_4])$	7.113(6)	7.860(5)	5.570(5)	90.11(8)	101.96(8)	105.89(7)
MC1-A Gt	$(Ca_{0.65}Mg_{1.25}Mn_{0.03}Fe_{1.07})^{[8]} Al_{2.00}^{[6]} [SiO_4]_3$	11.5583(14)					
MC1-A Cpx	$(Ca_{0.68}Na_{0.30})^{[8]} (Mg_{0.60}Fe_{0.08}Al_{0.33}Cr_{0.01})^{[6]} [Si_{1.94}Al_{0.06}O_6]$	9.9960(18)	8.52(2)	5.207(9)		106.1(2)	
MC1-A Amph	$(K_{0.14}Na_{0.47})^{[12]} (Na_{0.31}Ca_{1.58}Fe_{0.11})^{M4[8]} (Mg_{3.43}Fe_{0.52}Al_{0.98}Cr_{0.02}Ti_{0.05})^{M1,2,3[6]} [Al_{1.39}Si_{6.61}O_{22}] (OH)_2$	9.797(10)	17.93(2)	5.297(6)		104.85(9)	
RI Ru	$(Al_{1.97}Cr_{0.03})^{[6]} O_3$	4.7631(19)		12.999(14)			
RI Parag	$(K_{0.03}Na_{0.79})^{[12]} (Fe_{0.03}Mg_{0.06}Al_{1.92}Cr_{0.09}Ti_{0.01})^{[6]} [Al_{1.21}Si_{2.79}O_{10}] (OH)_2$	5.177(11)	9.03(3)	20.53(7)		95.0(2)	
RI Phlo	$(K_{0.62}Na_{0.28})^{[12]} (Fe_{0.30}Mg_{2.62}Al_{0.43}Cr_{0.11}Ti_{0.06})^{[6]} [Al_{1.33}Si_{2.67}O_{10}] (OH)_2$	5.310(12)	9.29(2)	20.44(2)		95.9(2)	
My Ru	$(Al_{1.99}Cr_{0.01})^{[6]} O_3$	4.7537(15)		12.980(5)			
My Ky	$(Al_{1.99}Cr_{0.01})^{[6]} [O/SiO_4]$	7.112(5)	7.842(6)	5.574(5)	90.08(7)	101.08(8)	105.88(6)
My Fu	$(K_{0.91}Na_{0.09})^{[12]} (Fe_{0.02}Mg_{0.02}Al_{1.80}Cr_{0.01}Ti_{0.09})^{[6]} [Al_{0.96}Si_{3.04}O_{10}] (OH)_2$	5.180(3)	8.992(6)	20.034(11)		95.80(5)	
Lon Ru	$(Al_{1.97}Cr_{0.03})^{[6]} O_3$	4.7613(19)		12.995(4)			
Lon Amph	$(K_{0.01}Na_{0.84})^{[12]} (Na_{0.02}Ca_{1.94}Fe_{0.04})^{M4[8]} (Mg_{2.80}Fe_{0.84}Al_{1.11}Cr_{0.22})^{M1,2,3[6]} [Al_{2.22}Si_{5.78}O_{22}] (OH)_2$	9.843(8)	17.970(8)	5.298(5)		105.22(8)	
OPXCPX Cpx	$(Ca_{0.86}Na_{0.11})^{[8]} (Mg_{0.82}Fe_{0.05}Al_{0.11}Cr_{0.05})^{[6]} [Si_{1.93}Al_{0.07}O_6]$						
OPXCPX Opx	$(Ca_{0.02}Mg_{1.73}Fe_{0.18}Al_{0.06}Cr_{0.02})^{[6]} [Si_{1.92}Al_{0.08}O_6]$						
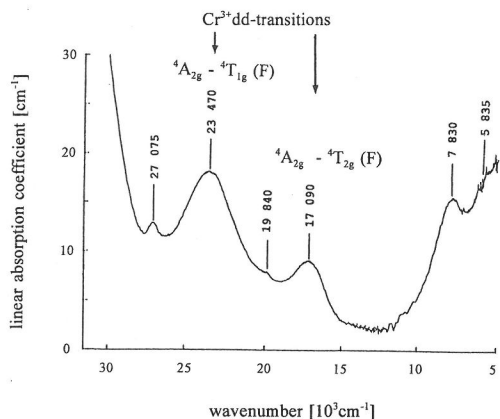
FIG. 2. Single crystal spectrum of the Cr^{3+}-bearing $(Pyr_{26}Gross_{49}Alm_{20})$-garnet ZagG1-Gt (*cf.* Tables 1 and 2) and assignment of the spin-allowed dd-transitions of Cr^{3+}[6]. Other bands in the UV/VIS and NIR ranges are dd-transitions of Fe^{2+}[8]. The crystal slab was 247 μm thick.

The other possible interpretation is to determine the baricenters of the two polarized components, derived from $(^4A_{2g} - ^4T_{2g})$, in the $E\|n_e$ and $E\|n_o$ spectra and to calculate the mean value. This then yields $10Dq_{cub}$ for the regular approach. In the case of corundum, the latter procedure yields $10Dq_{cub}$-values which are only 1.3% lower than those obtained in the first mentioned and, with respect to the symmetry, correct procedure.

Because a strict symmetry treatment is not possible in the case of the other minerals studied and as the deviation between the crystal field parameter as obtained in the strict vs. the cubic approach is small, the $10Dq_{cub}$-approximation is adopted for the evaluation of all the spectra measured in this study. If so, why are polarized and not unpolarized spectra used, which are more easily obtained? Such a procedure might produce erroneous $10Dq_{cub}$-values

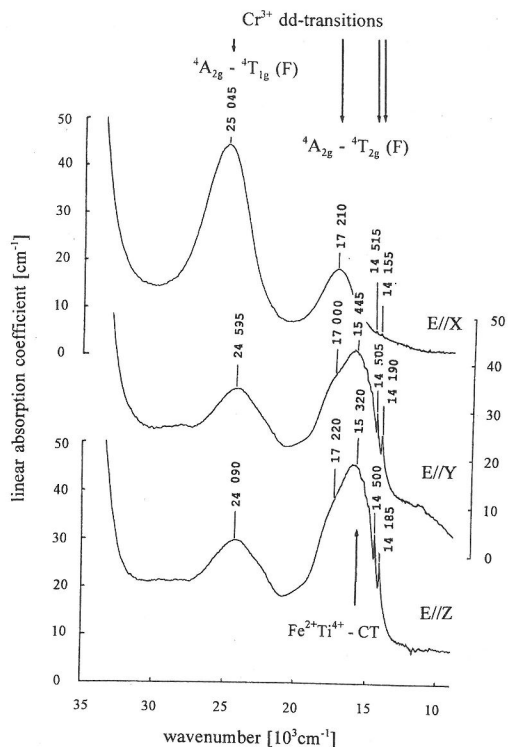transfer in edge-connected octahedra in the structure of this mineral (SMITH and STRENS, 1976).

As a consequence, the extraction of $10Dq_{Cr^{3+}}$-values necessary for our purpose of quantitatively checking CFC is a nontrivial problem and, hence, we ought to shortly comment on it for the Cr^{3+}-containing, coexisting minerals studied here.

Corundum—The trigonal field of the Cr^{3+}-centered octahedra yields two bands in the 10Dq-region at around 17900 and 18300 cm^{-1}, the first occurring in $E\|n_e$ and the second in $E\|n_o$ (*cf. e.g.* MCCLURE, 1958 and 1962). It is possible to base the interpretation of the spectra on a trigonal field approach (MCCLURE 1958; MACFARLANE, 1963) and to extract a trigonal field parameter $10Dq_{trig}$. In the case of all other minerals, the interpretation is based on the approximation of a regular octahedral field parameter $10Dq_{cub}$, because an exact treatment is impossible and, in any case, will not significantly enhance the accuracy of the crystal field parameter obtained. In case of corundum, this is obvious from the following consideration: We can recalculate $10Dq_{trig}$, obtained from the exact treatment for the point symmetry 3 of the corundum octahedra to the cubic field parameter by

$$Dq_{cub} = Dq_{trig} + \frac{7}{18} \times D\tau \qquad (8)$$

(KÖNIG and KREMER, 1977), wherein $D\tau$ is a parameter taking into account the trigonal distortion of the octahedra along C_3. $D\tau$ can be determined from the energies of all the transitions of Cr^{3+} in the corundum-spectra (KÖNIG and KREMER, 1977).

FIG. 3. Polarized single crystal spectra of the Cr^{3+}-bearing kyanite ZagG1-Ky (*cf.* Tables 1 and 2) and assignment of dd-transitions of Cr^{3+} as well as Fe^{2+}-Ti^{4+} charge-transfer. The two narrow low-energy bands of Cr^{3+} are due to spin forbidden transitions of this ion. Wavenumber positions of component bands are obtained by the curve fitting process (*cf.* text). Spectra E//X and E//Z are measured on a slab $\perp$Y (−Ky−3), 237 μm thick, the spectrum E//Y on a slab $\perp$Z (−Ky−1), 227 μm thick.
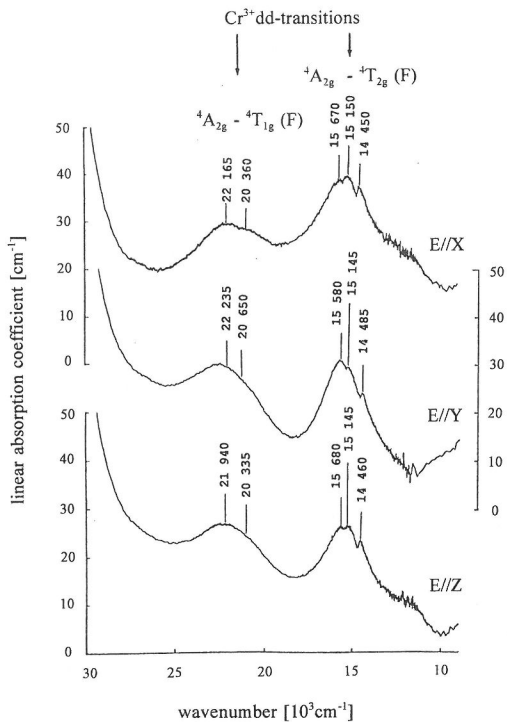
FIG. 4. Polarized single crystal spectra of the Cr^{3+}-bearing $(Jd_{45}Di_{47})$-clinopyroxene ZagG1-Kpx (cf. Tables 1 and 2). Baricenters of Cr^{3+} dd-transitions are indicated. Wavenumber positions of component bands are obtained by the curve fitting process. Spectra E//X and E//Y were measured on a slab ⊥Z (−Cpx−3), 110 μm thick, the E//Z spectrum on a slab X (−Cpx−5), 68 μm thick.

because the position of the baricenters depend on the polarization. Therefore, all three polarizations are needed, whereas an unpolarized spectrum of a crystal plate is a mixture of only two. Also, effect (iii) can only be identified, if present, on the basis of polarized spectra.

Garnet—The trigonal site distortion of the garnet octahedra incorporating Cr^{3+} is so small (NOVAK and GIBBS, 1971; ARNI *et al.*, 1985) that any band splitting that might result from effect (i) is indicated only by a slight asymmetry of the strong spin-allowed dd-bands of Cr^{3+}, even at low temperatures (TARAN *et al.*, 1994). Symmetry-related selection rules for the site symmetry $\bar{3}$ of the garnet octahedra are destroyed by the Ia3d symmetry of the overall structure. Hence, an evaluation based on the baricenters and yielding $10Dq_{cub}$ is in this case the only possible way to obtain the required data from the spectra, an example of which is shown in Fig. 2.

Kyanite—The spectra obtained (*e.g.* Fig. 3) ex-

hibit in the spectral region around 16000 cm^{-1}, where the $(^4A_{2g} - {}^4T_{2g})$-derived bands occur, a complex band system. This contains at least two strong and broad components, a high energy component at around 17200 cm^{-1}, polarized $\alpha_x < \alpha_y < \alpha_z$, and a low energy component at around 15500 cm^{-1}, which is not observed in the E∥X-spectrum and, in E∥Y and E∥Z, with $\alpha_y < \alpha_z$ polarization (Fig. 3). In addition, there occur two narrow bands between 14000 14500 cm^{-1}, caused by spin-forbidden transitions of Cr^{3+}, which show up with remarkably high intensity in kyanite (Fig. 3). These bands do not play a role in the extraction of $10Dq_{cub}$ and, therefore, will not be further commented upon here. The assignment of the strong component bands is based on the following results published so far:

(a) Pure, synthetic Cr^{3+}-bearing kyanites (LANGER and SEIFERT, 1971), with chromium-contents comparable to those of the natural kyanites studied here, show the $(^4A_{2g} - {}^4T_{2g})$-derived transition of Cr^{3+} at 16850 cm^{-1} in unpolarized powder remission spectra (LANGER, 1976). Single crystal spectra, of crystals with $n_{Cr^{3+}} = 0.3$ pfu, measured with E∥c and E⊥c which is close to the E∥Z and E∥X measurements of the present study, show the baricenter of this band at 16480 cm^{-1} with $\alpha_{\perp c} < \alpha_{\parallel c}$ polarization (LANGER, 1984 and 1988). Hence, the strong, high-energy component observed here is identified as the 10Dq-band of Cr^{3+}. We determined $10Dq_{cub}$ by averaging the baricenters of this component band as obtained by curve resolution of the three polarized spectra (Fig. 3).

(b) Most kyanites from metamorphic rocks, containing traces of chromium only, exhibit a typical blue color, the intensity of which is often undulous or zoned within the crystals. The polarized spectra of such kyanites were first obtained by WHITE and WHITE (1967) and are dominated by a strongly polarized, intense band system with maximum at 16000 cm^{-1}, absent in E∥X and with $\alpha_y > \alpha_z$. After an intense debate about the origin of these spectral features, it became obvious (SMITH and STRENS, 1976; PARKIN *et al.*, 1977) that the band system originates from Fe^{2+}-Ti^{4+} charge-transfer transitions in the c-parallel chains of edge-connected M(1)-, M(2)-octahedra of the structure (BURNHAM, 1963). Contributions of Fe^{2+}-Fe^{3+} charge-transfer in the low-energy wing of the band system do also contribute when chemistry and conditions of the kyanite formation allows for it. Because all features of the low-energy component band under discussion in our kyanite spectra corre-

spond to those of the Fe^{2+}-Ti^{4+} charge-transfer band identified in blue kyanites (*l.c.*), its assignment to charge-transfer of this type is obvious.

Clinopyroxene—The identification of the 10Dq-band in the spectra (*cf.* Fig. 4) and the extraction of $10Dq_{cub}$ of Cr^{3+} in the M(1)-octahedra of the clinopyroxene structure (CLARK *et al.,* 1969) pose no problems thanks to the spectral studies of ABS-WUMBACH *et al.* (1985) and of KHOMENKO and PLATONOV (1985). The baricenters of the ($^4A_{2g}$ − $^4T_{2g}$)-derived band system in E‖X, E‖Y and E‖Z polarization (Fig. 4) were determined and averaged to obtain $10Dq_{cub}$ in all clinopyroxenes of Table 1.

The only difficulty arose with the clinopyroxene exsolution from orthopyroxene, *i.e.* the spectra of the OPXCPX-Cpx sample in Table 1. Due to the (100) intergrowth of the clinopyroxene exsolution lamellae in the orthopyroxene matrix, the indicatrix of clinopyroxene is tilted against the face of the slab ‖ Y of orthopyroxene, corresponding to (100) within the error of the orientation. Therefore, the E-vector of the measuring radiation could only be approximately oriented parallel to X or Y of clinopyroxene in this case.

Orthopyroxene—Considering the radius of Cr^{3+} and the mean M-O distances within the octahedral M(1)- and M(2)-sites of the structure (CAMERON and PAPIKE, 1981), as well as the fairly weak distortion from regular geometry of M(1) as compared to M(2), it is to be expected that Cr^{3+} enters the former site, charge balance being achieved *e.g.* by $Al^{3+[4]}$ for $Si^{4+[4]}$ substitution. Entrance of chromium into the M(1)-sites of the orthopyroxene structure is confirmed by the evaluation of the polarized spectra of a synthetic Cr^{3+}-bearing enstatite (ROSSMAN, 1980). Thus, our evaluation of the spectra of OPXCPX-Opx (Table 1) is based on these results, $10Dq_{cub}$ being obtained as the average of the baricenters of the 10Dq-band in E‖X and E‖Z polarization. E‖Z could not be measured on this sample (see above), and, in this polarization, the baricenter of the 10Dq-band system occurs at slightly higher wavelengths, *i.e.* lower energies compared to the two former polarizations (ROSSMAN, 1980). Therefore, the $10Dq_{cub}$-value obtained here may be too high by about 100 cm^{-1}, which would correspond, in $CFSE_{Cr^{3+}}$, to +1.4 kcal/g-atom$_{Cr^{3+}}$.

Clinoamphiboles, dioctahedral and trioctahedral micas—The 10Dq-band system in the spectra obtained on the clinoamphiboles of Tables 1 and 2 exhibits, if any, only a very weak low-symmetry splitting and also weak polarization with $\alpha_Y > \alpha_X \cong \alpha_Z$. Hence, Cr^{3+} is incorporated in octahedral sites that are only slightly distorted from regular

geometry. This is the case for the M(1,2,3) sites of the structure (*e.g.*, PAPIKE *et al.,* 1969), which are, therefore, assumed to incorporate chromium.

There is no information in the literature about the distribution of Cr^{3+} in trioctahedral biotite or dioctahedral muscovite and paragonite that can help in the interpretation of the spectra of our samples RI Phlo, My Fu and RI Parag (Tables 1 and 2). Effects (i) and (ii) are not observed in the case of RI Phlog; low band intensity may be a consequence of the low Cr^{3+}-concentration in this sample (Table 2). My Fu and RI Parag, with pleochroic schemes $\alpha_Y \cong \alpha_Z < \alpha_X$ and $\alpha_Y < \alpha_Z \ll \alpha_X$, respectively, of the 10Dq-band system, do not show any low symmetry splitting although band intensities are strong enough to detect it. In any case, Cr^{3+} will preferentially enter the octahedral sites with lowest distortion from regular geometry, *i.e.* in phlogopite the M(1)-sites with trans-configuration of the two OH-groups. FAYE (1968), in his interpretation of the spectra of a fuchsite from Madagaskar, considers the M(2)-position with cis-configuration of OH to be "relatively distorted," whereas the M(1)-position, normally vacant in dioctahedral micas, is close to regular geometry (*e.g.*, BAILEY, 1984).

Due to very weak band intensity and a possible polarization $\alpha_Y \cong \alpha_Z \ll \alpha_x$, the 10Dq-band in RI Phlo could only be obtained from the E‖X spectrum, which bears on the accuracy of $CFSE_{Cr^{3+}}$ for this coexisting mineral. In case of the dioctahedral micas, $10Dq_{cub}$ was calculated from the baricenters for all three polarizations.

In summary—The spectral results on Cr^{3+} in the various coexisting minerals studied here, as well as the considerations about their evaluation, lead to values of $10Dq_{cub}$ and these to values of $CFSE_{Cr^{3+}}$ as listed in columns 2 to 4 of Table 3. $10Dq_{cub}$ values are estimated to be correct to within about ±30 cm^{-1}, corresponding to ±0.43 KJ/g-atom for the values of $CFSE_{Cr^{3+}}$, except for OPXCPX and RI Phlo as discussed before.

The choice of concentration unit

When Cr^{3+} partitions between different phases of a system, a common concentration unit, valid for all the phases, must be chosen. Thus, wt% Cr_2O_3 or mol% Cr^{3+}-end member in the respective solid solution are inappropriate as they relate the Cr^{3+}-concentration to the very phase just under consideration. Therefore, the concentrations must be recalculated to a unit volume, *e.g.* 1dm^3 or l, of all the phases studied. This is achieved by

$$C_{Cr^{3+}[g-atom/l]} = n_{Cr^{3+}}/V_M \qquad (9)$$

wherein $n_{Cr^{3+}}$ are Cr^{3+}-ions per formula unit of the

respective crystallochemical formulae of the minerals and V_M their molar volumes in dm^3 as obtained from eqn. (7). The values of V_{el}, as obtained from the X-ray diffraction data, of V_M, $n_{Cr^{3+}}$ and, finally, of $c_{Cr^{3+}}$ in g-atom/l are compiled in columns 5 to 8 of Table 3. The error in $c_{Cr^{3+}}$, resulting from the uncertainties in the determination of V_{el} and of Cr^{3+}-analyses by microprobe, is given in parentheses.

CRYSTAL FIELD STABILIZATION AND INTERCRYSTALLINE PARTITIONING OF CR^{3+}—THE CONCLUSIONS

Figure 5 shows a plot of the uniformly normalized Cr^{3+}-concentrations, $C_{Cr^{3+}}$[g-atom/l], as a function of the crystal field stabilization energy, $CFSE_{Cr^{3+}}$, that the chromium ions gain in their respective structural matrix. From this figure, it is obvious that there exists a positive, quantitative correlation between the two quantities, as postulated by eqn. (5), the function f being of the same type for all the parageneses studied. The only exception, OPXCPX, may be explained by a value of CFSE that is too high in the case of orthopyrox-

ene (see above). Crystallochemical peculiarities involved in the Cr^{3+}-substitutions based on $Ca_{M2}Mg_{M1} \ll Na_{M2}Cr_{M1}$ in clinopyroxene and on $M_{M1}Si_T \ll Cr_{M1}Al_T$ in orthopyroxene, whereby the additional presence of significant amounts of Fe^{2+} in the latter phase may also be of influence for the exceptional sample.

Calculating $K_{D,Cr^{+3}}$-values and plotting them as a function of the difference of the crystal field stabilization energies of the respective two phases Ph1 and Ph2 (Fig. 6), also shows positive correlations for the various parageneses, except for OPXCPX with a slightly negative K_D.

From this it is obvious that the data obtained show a quantitative, positive correlation between Cr^{3+} [g-atom/l] and $CFSE_{Cr^{3+}}$, as predicted by CFC, except for a clinopyroxene exsolution in orthopyroxene, a deviation that may be explained by possible errors of the $10Dq_{cub}$-determination and crystallochemical peculiarities of the substitutions in this case.

This proves the CFC concept to be valid, at least for Cr^{3+}-concentrations above the trace level.

Table 3. Crystal field splitting, $10Dq_{Cr3+}$, crystal field stabilization enrgy, $CFSE_{Cr3+}$, and concentration of chromium, c_{Cr3+} in [g-atom/l], in the parageneticminerals studied. V_{el}, V_M and n_{Cr3+} are the unit cell volume, molar volume and atoms per formula unit, respectively. [a] the extraction of 10Dq is discussed in the text. [b] The M(1,2,3) positions are taken into account (cf. text).

| Crystals (cf. Tab 1)	$10Dq_{Cr3+}$ [1] $[cm^{-1}]$	$CFSE_{Cr3+}$ $[cm^{-1}]$	$CFSE_{Cr3+}$ [KJ/g-atom]	V_{el} $[A^3]$	V_M $[dm^3/mole]$	n_{Cr3+}	c_{Cr3+} [g-atom/l]
Zag C1-Gt	17 030	20 435	244.5	1600.5(1.6)	0.1190(1)	0.093	0.77 (3)
Zag C1-Cpx	15 340	18 408	220.2	428 (4)	0.0644(6)	0.027	0.418(18)
Zag-C1.Ky	17 100	20 520	245.5	293.6 (4)	0.0442(1)	0.045	1.09 (9)
Zag G1-Gt	17 090	20 510	245.3	1600.5(1.6)	0.1190(1)	0.076	0.63 (3)
Zag G1-Cpx	15 265	18 318	219.1	428 (4)	0.0644(6)	0.023	0.36 (2)
Zag G1-Ky	17 145	20 579	246.1	293.6 (4)	0.0442(1)	0.042	0.94 (7)
MC1-A Gt				1544.1 (5)	0.1162(1)	0.001	
MC1-ACpx	15 435	18 522	221.6	424.2(1.3)	0.0639(2)	0.019	0.14 (2)
MC1-A Amph	15 200	18 240	218.2	899.4(1.5)	0.2708(5)	0.024	0.089(15)[b]
RI Ru	18 130	21 756	260.3	255.4	0.0256(1)	0.029	1.12 (6)
RI Parag	16 605	19 926	238.4	957 (5)	0.1441(8)	0.088	0.61 (4)
RI Phlo	16 695	20 034	239.3	1002 (4)	0.1509(6)	0.113	0.75 (4)
My Ru	18 140	21 768	260.4	254.0(2)	0.0255(1)	0.011	0.44 (2)
My Ky	17 150	20 580	246.6	293.0(4)	0.0441(3)	0.009	0.204(17)
My Fu	16 255	19 506	233.3	928.3(9)	0.1398(1)	0.014	0.100(4)
Lon Ru	18 100	21 720	259.8	255.1(1)	0.0265(1)	0.025	0.98 (6)
Lon Amph	15 550	18 636	222.9	904.2(1.2)	0.2723(3)	0.217	0.80 (3)
OPXCPX-Cpx	15 640	18 768	224.5	440 (10)	0.062(15)	0.046	0.70 (4)
OPXCPX-Opx	15 900	19 085	228.3	830 (10)	0.0625(7)	0.023	0.37 (5)
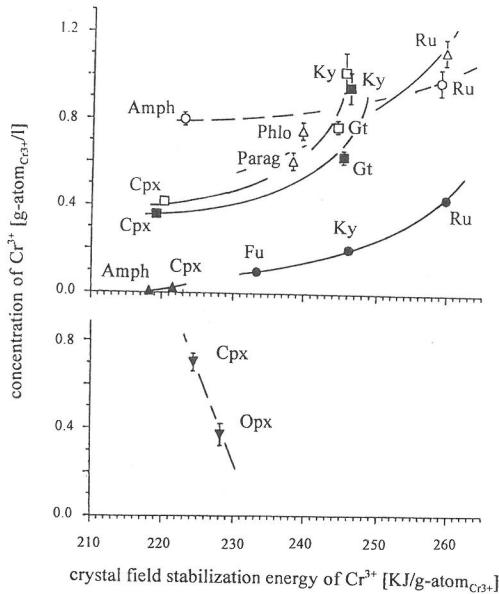
FIG. 5. Plot of the Cr^{3+}-concentration, normalized to the volume unit for all minerals studied (*cf.* text), $c_{Cr^{3+}}$ versus the $CFSE_{Cr^{3+}}$ in their structure. The different symbols represent the various parageneses studied: C1, G1, MC1-A, RI, My, Lon, OPXCPX (*cf.* Table 1); abbreviations as in Table 1.
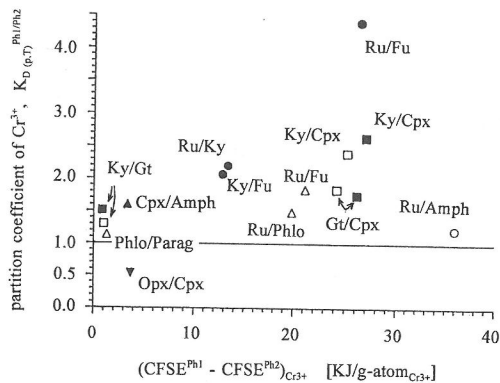

FIG. 6. Partition coefficient $K_{D,Cr3+,(p,T)}^{Ph1/Ph2}$ as a function of the difference of the crystal field stabilization energy of chromium in the respective two phases $CFSE^{(Ph1-Ph2)}$. Symbols and abbreviations as in Fig. 5.

REFERENCES

ABS-WURMBACH I., LANGER K. and OBERHÄNSLI R. (1985) Polarized absorption spectra of single crystals of the chromium bearing clinopyroxenes kosmochlore and Cr-aegirine-augite. *N. Jb. Miner. Abh.* **152,** 293–319.

ANDRUT M. (1995) Kristallfeldstabilisierungsenergie und interkristalline Verteilung von Übergangsmetallionen in silikatischen Paragenesen. Dr.-Dissertation, Technische Universität Berlin, 123 pp.

ARNI R., LANGER K. and TILLMANNS E. (1985) Mn^{3+} in garnets. III. Absence of Jahn-Teller distortion in synthetic Mn^{3+}-bearing garnet. *Phys. Chem. Minerals* **12,** 279–282.

BAILEY S. W. (1984) Crystal chemistry of the true micas. In *Micas* (ed. S.W. BAILEY). *Rev. in Mineral.* **13,** pp. 13–60, Mineralogical Society of America.

BLOSS F. D. (1981) *The spindle stage: Principles and practice.* Cambridge University Press, Cambridge.

BURNHAM C. W. (1963) Refinement of the crystal structure of kyanite. *Z. Kristallogr.* **118,** 337–360.

BURNS R. G. (1968) Enrichments of transition metal ions in silicate structures. In *Symposion on the origin and distribution of elements, Section 5: Terrestrial abundances* (ed. T.H. AHRENS). Pergamon Press, New York, 1151–1164.

BURNS R. G. (1970a) Crystal field spectra and evidence for cation ordering in olivine minerals. *Amer. Mineral.* **55,** 1608–1632.

BURNS R. G. (1970b) *Mineralogical applications of crystal field theory.* Cambridge University Press, Cambridge.

BURNS R. G. (1976) Partioning of transition metals in mineral structures in the mantle. In *The physics and chemistry of minerals and rocks* (ed. R. G. J. STRENS). Wiley, New York, 555–572.

BURNS R. G. (1993) *Mineralogical applications of crystal field theory.* Cambridge University Press, Cambridge, 2nd ed.

BURNS R. G., CLARK J. R. and FYFE W. S. (1964) Crystal field theory and applications to problems in geochemistry. In *Chemistry of the earth's crust* (ed. V. VINOGRADOV). *Proc. Vernadsky Centen. Symp.* **2,** 88–106.

BURNS R. G. and FYFE W. S. (1964) Site preference energy and selective uptake of transition metal ions during magmatic recrystallization. *Science* **144,** 1001–1003.

BURNS R. G. and FYFE W. S. (1966) Distribution of elements in geological processes. *Chem. Geol.* **1,** 49–56.

BURNS R. G. and FYFE W. S. (1967a) Trace element distribution rules and their significance. *Chem. Geol.* **2,** 89–104.

BURNS R. G. and FYFE W. S. (1967b) Crystal field theory and the geochemistry of transition elements. In *Researches in Geochemistry* (ed. P.H. ABELSON), Wiley, New York.

Burns, R. G. and Sung C. M. (1978) The effect of crystal field stabilization on the olivine-spinel transition in the system Mg_2SiO_4-Fe_2SiO_4. *Phys. Chem. Minerals* **2**, 349–364.

Cameron M. and Papike J. J. (1981) Structural and chemical variations in pyroxenes. *Amer. Mineral.* **66**, 1–50.

Clark J. R., Appleman D. E. and Papike J. J. (1969) Crystal chemical characterization of clinopyroxenes based on eight new structure refinements. *Min. Soc. Amer., Spec. Pap.* **2**, 31–50.

Cotton A. F. (1971) *Chemical applications of group theory.* Wiley, New York.

Curtis D. C. (1964) Applications of the crystal field theory to the inclusions of trace transition elements in minerals during magmatic differentiation. *Geochim. Cosmochim. Acta* **28**, 389–402.

Dunn T. M., McClure D. S. and Pearson R. G. (1965) *Some aspects of crystal field theory.* Harper & Row, New York.

Faye G. H. (1968) Optical spectra of certain transition metal ions in muscovite, lepidocrocite and fuchsite. *Can. J. Earth Sci.* **5**, 31–38.

Jensen B. B. (1973) Patterns of trace element partitioning. *Geochim. Cosmochim. Acta* **37**, 2227–2242.

Khomenko V. M. and Platonov A. N. (1985) Electronic absorption spectra of Cr^{3+}-ions in natural pyroxenes. *Phys. Chem. Minerals* **11**, 261–265.

König E. and Krämer S. (1977) *Ligand field energy diagrams.* Plenum Press, New York.

Langer K. (1976) Synthetic 3d-transition metal bearing kyanites $(Al_{2-x}M_x)SiO_5$. In *The physics and chemistry of minerals and rocks* (ed. R. G. J. Strens). Wiley, New York, 389–402.

Langer K. (1984) Die Farbe von Mineralen und ihre Aussagefähigkeit für die Kristallchemie. *Rhein. Westfäl. Akad. Wiss., Vortr.* N332, 7–60.

Langer K. (1988) UV to NIR spectra of silicate minerals obtained by microscope spectrometry and their use in mineral thermodynamics and kinetics. In *Physical properties and thermodynamic behaviour of minerals* (ed. E. K. H. Salje). Reidel, Dordrecht, 639–685.

Langer K. and Frentrup K.R. (1979) Automated microscope-absorption-spectrophotometry of rock-forming minerals in the range 40,000–5,000 cm⁻¹ (250–2,000 nm). *J. Microscopy* **116**, 311–320.

Langer K. and Seifert F. (1971) High pressure-high temperature synthesis and properties of chromium kyanite, $(Al,Cr)_2SiO_5$. *Z. anorg. allg. Chem.* **383**, 29–39.

Lever A. B. P. (1968) *Inorganic electronic spectroscopy.* Elsevier, Amsterdam.

MacFarlane R. M. (1963) Analysis of the spectrum of $3d^3$ ions in trigonal crystal field. *J. Chem. Phys.* **39**, 3118–3126.

McClure D. (1958) Electronic spectra of molecules and ions in crystals. *Solid State Phys.* **8**, 1–47.

McClure D. (1962) Optical spectra of transition metal ions in corundum. *J. Chem. Phys.* **36**, 2757–2768.

Merlino S. (1965) Applicazione delle teoria del campo cristallino allo studio della ripartizione di elementi in tracce. *Atti della Soc. Tosc. Sci. Nat., Ser. A,* **72**, 14 pp.

Novak G. A. and Gibbs G. V. (1971) The crystal chemistry of the silicate garnets. *Amer. Mineral.* **56**, 791–825.

Papike J. J., Ross M. and Clark J. R. (1969) Crystal chemical characterization of clinoamphiboles based on five new structure refinements. *Min. Soc. Amer., Spec. Pap.* **2**, 117–136.

Parkin K. M., Loeffler B. M. and Burns R. G. (1977) Mössbauer spectra of kyanite, aquamarine and cordierite showing intervalence charge transfer. *Phys. Chem. Minerals* **1**, 301–311.

Rossman G. R. (1980) Pyroxene spectroscopy. In: *Pyroxenes* (ed. C. T. Prewitt) *Rev. in Mineral.* **7**, pp. 91–115, Mineralogical Society of America.

Schläfer H. L. and Gliemann G. (1980) *Einführung in die Ligandenfeldtheorie.* Akademische Verlagsgesellschaft, Frankfurt, 2nd ed.

Schwartz H. P. (1976) The effect of crysatl field stabilization on the distribution of transition metals between metamorphic minerals. *Geochim. Cosmochim. Acta* **31**, 503–517.

Shimura Y. and Tsuchida R. (1956) Absorption spectra of Co(III) complexes. II. Redetermination of the spectrochemical series. *Bull. Chem. Soc. Japan* **31**, 311–316.

Smith G. and Strens R. G. J. (1976) Intervalence-transfer absorption in some silicate, oxide and phosphate minerals. In *The physics and chemistry of minerals and rocks* (ed. R. G. J. Strens), Wiley, New York, 583–612.

Strens R. G. J. (1968) Stability of the Al_2SiO_5 solid solutions. *Mineral. Mag.* **36**, 839–849.

Tanabe Y. and Sugano S. (1954a) On the absorption spectra of complex ions. I. *J. Phys. Soc. Japan* **9**, 753–766.

Tanabe Y. and Sugano S. (1954b) On the absorption spectra of complex ions. II. *J. Phys. Soc. Japan* **9**, 767–779.

Taran M. N., Langer K., Platonov A. N. and Indutny V. V. (1994) Optical absorption investigation of Cr^{3+}-bearing minerals in the temperature range 77–797 K. *Phys. Chem. Minerals* **21**, 360–372.

Tröger W. E. (1952) *Tabellen der gesteinsbildenden Minerale.* Schweizerbart, Stuttgart.

Tsuchida R. (1938a) Absorption spectra of coordination compounds. I. *Bull. Chem. Soc. Japan* **13**, 388–400.

Tsuchida R. (1938b) Absorption spectra of coordination compounds. II. *Bull. Chem. Soc. Japan* **13**, 436–450.

Tsuchida R. (1938c) Absorption spectra of coordination compounds. III. Special bands of Cr^{3+}-complexes. *Bull. Chem. Soc. Japan* **13**, 471–480.

White E. W. and White W. B (1967) Electron microprobe and optical absorption study of colored kyanites. *Science* **158**, 915–917.

Williams R. J. P. (1959) Deposition of trace elements in basic magma. *Nature* **184**, 44.

Wilson E. B., Decius J. C. and Cross P. C. (1955) *Molecular vibrations - The theory of infrared and Raman spectra.* McGraw-Hill, New York.